

## PREPARATION AND CORROSION RESISTANCE OF EPOXY RESIN COATING WITH DOPAMINE MODIFIED BASALT FIBER

X. YU<sup>a,\*</sup>, Q. WU<sup>b</sup>, R. CHEN<sup>b</sup>, J. WANG<sup>b</sup>

<sup>a</sup> School of Additive Manufacturing, Zhe Jiang Institute of Mechanical & Electrical Engineering, Hangzhou, China, 310053

<sup>b</sup> College of Materials Science and Chemical Engineering, Harbin Engineering University, Harbin, China, 150001

Herein, the anti-corrosion properties of basalt fiber materials modified by bio-stimulation, which grows poly-dopamine in situ on the fiber surface by a chemical modification method. This approach not only triggers cross-linking reaction between the modifier and the resin during the curing process of resin, to form a body type network structure that is closely connected and runs through the whole curing system, but also enhances the interaction between modifier and epoxy resin. The electrochemical test revealed that the corrosion resistance of the composite coating is greatly improved by 21% compared to the pure epoxy coating.

(Received July 19, 2020; Accepted November 5, 2020)

*Keywords:* Basalt fiber, Surface modification, Composite coating, Corrosion resistance

### 1. Introduction

Epoxy resin has a wide utilization in coatings, electronic appliances, composite materials, adhesives and many other fields because of the characteristics of high mechanical properties, compact molecular structure, excellent bonding performance, outstanding insulation and good heat resistance. [1-5] In recent years, its high performance-price ratio has encouraged development. However, the traditional epoxy resin also has some inherent shortcomings, such as low curing activity, difficulty in curing at room temperature, anti-adhesion of cured paint film, poor adhesion and so on. [6-8] With the increasing production capacity and demand, many people have carried out extensive research to meet the increasingly complex demand, hoping to find new methods to improve the properties of resin. Epoxy composite coatings taking inorganic fibers as reinforcing phase have been attracted much attention due to their compact structure, wear resistance and good corrosion resistance. [9-10] However, some kinds of inorganic fibers are rigid materials rather than ductile materials; they are not only unable to effectively reduce the impact force when subjected to impact, but also easy to form an internal reaction leading to a peeling of the coating.

The basalt fiber can improve the mechanical and corrosion resistance of the composite coating. [11-14] Therefore, the basalt fiber with low dielectric constant is selected as toughening material of the anti-corrosion coating. [15,16] The properties of coatings can be greatly improved in terms of wear resistance, corrosion resistance and toughness by using modulus polymer of excellent wear resistance and super high elasticity. Experiments have proved that there will be many defects in the coatings if basalt fibers are directly added into the composite coatings during the preparation process because of the uneven size and easy agglomeration. [17-22] Therefore, the modification of basalt fibers is a key point of the coating preparation. [23, 24] Ma reported that BF was impregnated

---

\* Corresponding author: yygdupt\_mmc@126.com

with La-EDTA to improve its mechanical and interfacial properties, the measurement results confirm the applicability of La-EDTA BF as a reinforcement for BADCy composites. [25] S. Ezhil Vannan prepared copper coating by using copper sulphate solution on the basalt short fibers to avoid any interface reactions. [26] These results indicate that basalt fibers are potential inorganic fibers for interfacial effects and corrosion prevention.

For a long time, scientists have been hoping that the interface of treated inorganic substance and resin is a flexible deformable phase to alleviate the interfacial stress caused by the different shrinkage between resin and filler in the curing process of composite coatings. [27- 29] According to the properties of reinforced composites, a restraint layer at the interface is needed to obtain the maximum adhesion and hydrolysis resistance. The mechanism of KH570 in this paper is more inclined to the latter. [30] Dopamine has already become a kind of new coating material development trend that more and more people have paid close attention to. [31-34] The main advantage of dopamine is that it can polymerize and adhere to almost all substrates under very mild conditions and humid environment. The dopamine layer with hydroxyl and imide groups can be deposited as a bridge for further functionalization. Therefore, the combination of biomimetic dopamine adhesion and inorganic material modification will be a widely used surface modification method. [35]

In this study, to improve the interfacial properties of BF and EP without degrading the mechanical properties of composite coating, PDA-KH570@BF-E51 was prepared by impregnation. The weather ability of the fiber reinforced resin can be improved by grafting continuous and dense biomimetic dopamine layer on the surface of basalt fiber treated with silane coupling agent. Moreover, by investigating the structure–property relationship, the origin of the change in the wetting and mechanical properties of BF were determined. The experimental results show that the properties of composite coatings are closely related to the relative content of resin and fiber, and mainly depend on the bonding strength of the composite interface between fibers and matrix resins. In addition, the bonding strength between coatings and substrates also plays an important role. Accordingly, the interface strength between basalt fiber and matrix resin is an important factor affecting the coating properties.

## 2. Materials and methods

### 2.1. Materials

Basalt chopped fiber with diameter of 5 mm come from Shandong Juyuan Basalt Fiber Co, Ltd. Table 1 shows the element of short-cut basalt fiber. Acetone ( $\text{CH}_3\text{COCH}_3$ ), ethanol ( $\text{C}_2\text{H}_5\text{OH}$ ) comes from Tianjin Fuyu Fine Chemical Co., Ltd., tris (hydroxymethyl) carbamate (Tris-HCl buffer solution (0.05mol/L, 25 °C ), Tris (hydroxymethyl) aminomethane, dopamine hydrochloride ( $\text{C}_8\text{H}_{11}\text{N}_2 \text{HCl}$ ) comes from Aladdin reagent limited. Company, KH570 is provided by Shanghai Zhongyi Plastic Products Factory China.

Table 1. Chemical element of short basalt fiber.

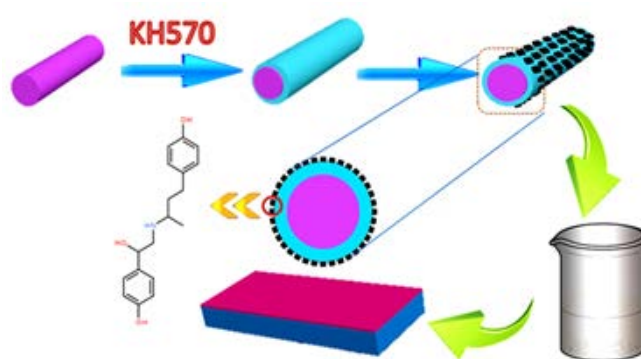
Element	$\text{SiO}_2$	$\text{Al}_2\text{O}_3$	$\text{Fe}_x\text{O}_y$	MgO	CaO
Wt %	69.51	14.18	3.92	2.41	5.62

### 2.2. Method

*Preprocessing of fibers:* Firstly, the short-cut basalt fibers were rinsed successively with DI water and ethanol, and then the pe-dispersion by ultrasonic vibration improved the dispersion of fibers apparently. After that, the fibers were pretreated with acetone in a Soxhlet extractor for 12 hours to remove impurities and organic reagents from the fibers, finally, they were processed in a small crusher.

*Preparation of KH570-PDA-BF:* With anhydrous ethanol as solvent, KH570 solution with 1 % mass fraction is made, in which the pretreated short basalt fiber then will be dissolved. In this process, the alkoxy (R'O-) at one end of silane (KH570) hydrolyzes into silicyl (Si-OH) that can react with silicon hydroxyl on BF surface. The reaction then forms covalent bonds or hydrogen bond and a chemical bond "Bridges" accordingly on the surface, which is advantageous to the grafting of macromolecule (PDA). Specific process refers to scheme1. Stir the KH570@BF for 8 hours under sealed magnetic stirring at 80 °C, then wash it with anhydrous ethanol and dry for 12 hours. After that, prepare the Tris-HCl buffer solution with a pH of 7.5 and add C<sub>8</sub>H<sub>11</sub>NO<sub>2</sub>HCl and KH570-BF at a ratio of 1:10 into it. After magnetic stirring for 24hours, KH570-PDA-BF is prepared.

*Pretreatment of Q235 carbon steel:* Firstly, the mixture of a certain proportion of hydrochloric acid, glacial acetic acid and distilled water was used to treat Q235 carbon steel to remove the rust and oxides on the surface of the carbon steel. Then, rinsed off the treatment agent quickly by using anhydrous ethanol, and dried it quickly by using cool air of the hair dryer to avoid the redox reaction on the surface.



*Schematic 1. Representations of the preparation process of the composite coating.*

*Preparation of composite coatings:* The coating is prepared by blending method as shown in Schematic 1. The composite particles are blended with resin solution at the ratio of 5%, 10%, 15% and 20%. Previously, the grinded PDA-KH570@BF is firstly dispersed by ultrasound with anhydrous ethanol and then mixed with epoxy resin E51 in sequence. After that, add defoaming agent into the mixture and stir for 1h. Then coat it on Q235 carbon steel by rotary coating method after 5 hours and finally seal the treated Q235 carbon steel at room temperature for 7 days.

*Characterization:* The microstructures of original BF and modified BF were observed by the SEM system (Hitachi SU-8010, Tokyo, Japan). Furthermore, the fracture surfaces of the impact specimens were also investigated by this apparatus. On the purpose of ensuring availability and accuracy of the data, a golden layer was plated on the scanning surfaces to avoid charging under the electron beam, which would affect the measurement results. The elemental compositions of the samples were studied by Energy Dispersive Spectrometer (EDS). Fourier transform infrared spectroscopy (FTIR) analysis was performed on Spectrum 100 of PerkinElmer with the wavenumber range of 4000–400 cm<sup>-1</sup>. Each spectrum was obtained by adding 64 consecutive scans with a resolution of 4 cm<sup>-1</sup>. The specimens were thin films (about 70 μm thick) prepared by hot pressing in a hydraulic press. The crystal phase and structure information of the samples were studied by X-ray powder diffraction (XRD) diffractometer (Rigaku TTR-III). X-ray photoelectron spectroscopy (XPS) analysis was performed on PHI 5700 electron spectrometer with Al K<sub>α</sub> radiation. The electrochemical impedance spectroscopy (EIS) is obtained from a electrochemical workstation (Metrohm PGSTAT 302N) of three-electrode system in this paper. This system uses coated soft steel as working electrode while saturated calomel electrode (SCE) and platinum foil as reference electrode and counter electrode respectively. And the experiment is carried out under an open circuit potential (OCP) of frequencies ranging from 10 kHz to 10 MHz.

### 3. Results and discussion

The scanning electron microscope image in Fig. 1 shows that the prepared particles have flake-like morphology. The substance in the yellow frame is PDA. With the increase of reaction time, more and more lamellar structures are formed. Finally, a uniform array distribution is formed on the surface of the fibers, the flake-like structure is about 100-200 nm. As shown in Fig. 2, EDS analyses is performed to compare the morphological and compositional changes on the BF surface before and after modification.

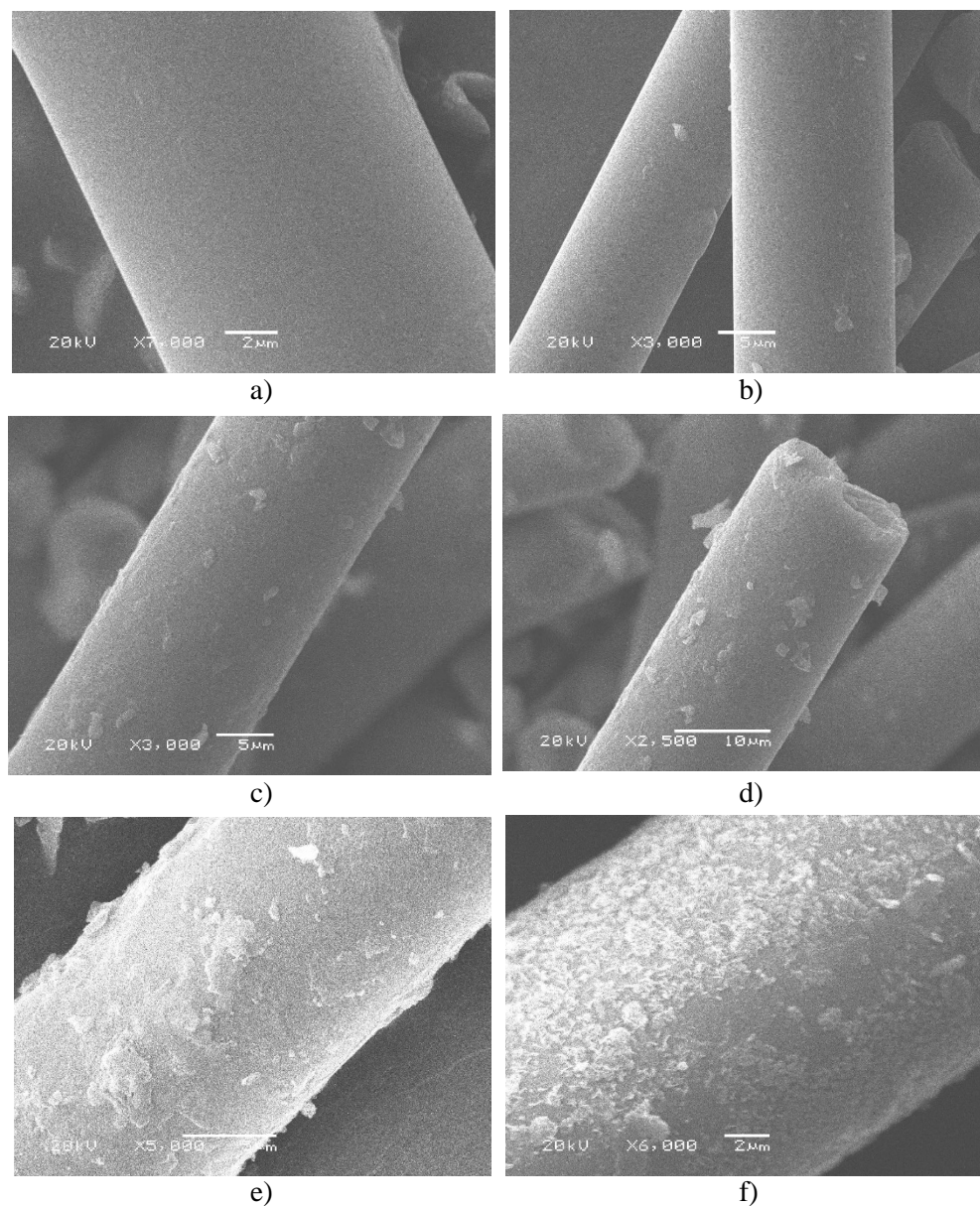


*Fig. 1. SEM images of (a) KH570@BF. PDA-KH570@BF with different reaction time: (b) 2h; (c) 6h; (d) 12h; (e) 18h; (f) 24h.*

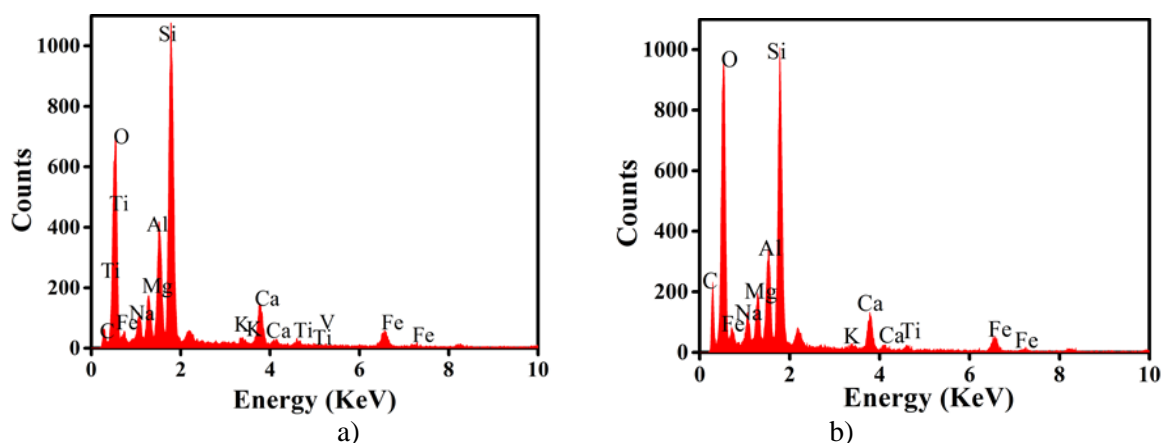


Fig. 2. (a) and (b) represent the EDS profiles of pristine BF and PDA- KH570@BF.

In order to evaluate the chemical interaction between functional groups and to determine the relative change of chemical structure, the FTIR analysis was carried out. **Figure 3** shows the FTIR spectra of BF, KF and P-K@F. The results prove once again the reaction to some extent. The broad peaks observed at  $2916\text{ cm}^{-1}$  and  $2850\text{ cm}^{-1}$  were assigned to vibrational absorption peaks of methyl and methylene; [35] Moreover, the absorption peak at  $1100\text{ cm}^{-1}$  to  $1500\text{ cm}^{-1}$  demonstrated that there were KH570 growing in situ on the sample, which were the characteristic peaks of the stretching vibration peak of C=O, the symmetric and anti-symmetric stretching vibration of  $-\text{CH}_3$  of KH570, confirming the successful modification of KH570 in based fibre through in-situ polymerization technique[36].

Table 2. EDS analysis of PDA- KH570@BF and pristine BF.

Elements	Pristine BF (wt %)	PDA- KH570@BF (wt %)	Increment (wt %)
C	26.01	54.26	108.61%
O	42.63	29.33	-31.20%
Al	7.01	3.39	-51.64%
Si	18.82	9.46	-49.73%
Fe	5.53	3.35	-39.42%

XPS analysis was conducted to ascertain the chemical changes on the surface of modified basalt fiber are shown in Fig. 4. Although basalt fibers contain no carbon, more than half of the fibers have carbon bonds on their surfaces. The C 1s XPS spectrum of KH570-BF is decomposed in Fig. 4c. Among them, where three components are contributed by C-C/C-H ( $284.38\text{ eV}$ ), C-C=O ( $285.98\text{ eV}$ ), and C-O/O-C=O ( $288.08\text{ eV}$ ), characteristic peaks of adventitious carbon, these are different carbon states of KH570 [37-39].

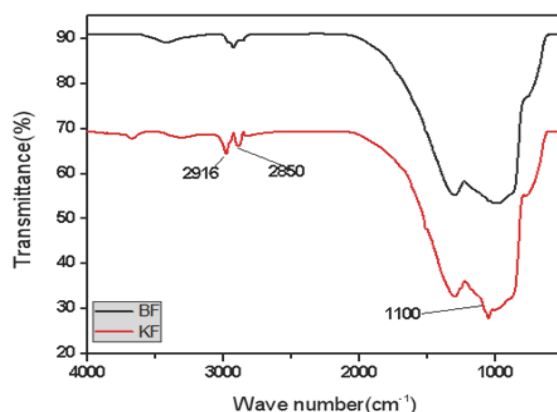


Fig. 3. FT-IR spectra of BF before and after modification.

Therefore, we can believe KH570 exists on the surface of fiber, which further convinces that KH570 was chemically grafted on the surface of BF. Two signals representing N 1s emerged in the spectra of the P-K@BF (Fig. 5d), confirming the presence of nitrogen on the surface of the sample and the successful in-situ polymerization of PDA on the fiber surface. Those results above proved that after modification, -COOH and more -OH were introduced onto the BF surface and electrons were transferred during the replacement process, so that the content of C-O/C-OH was more than double that of original fiber, indicating that there might be an enhanced bonding environment, which provided conditions for improving the performance of combination between BF and epoxy resin.

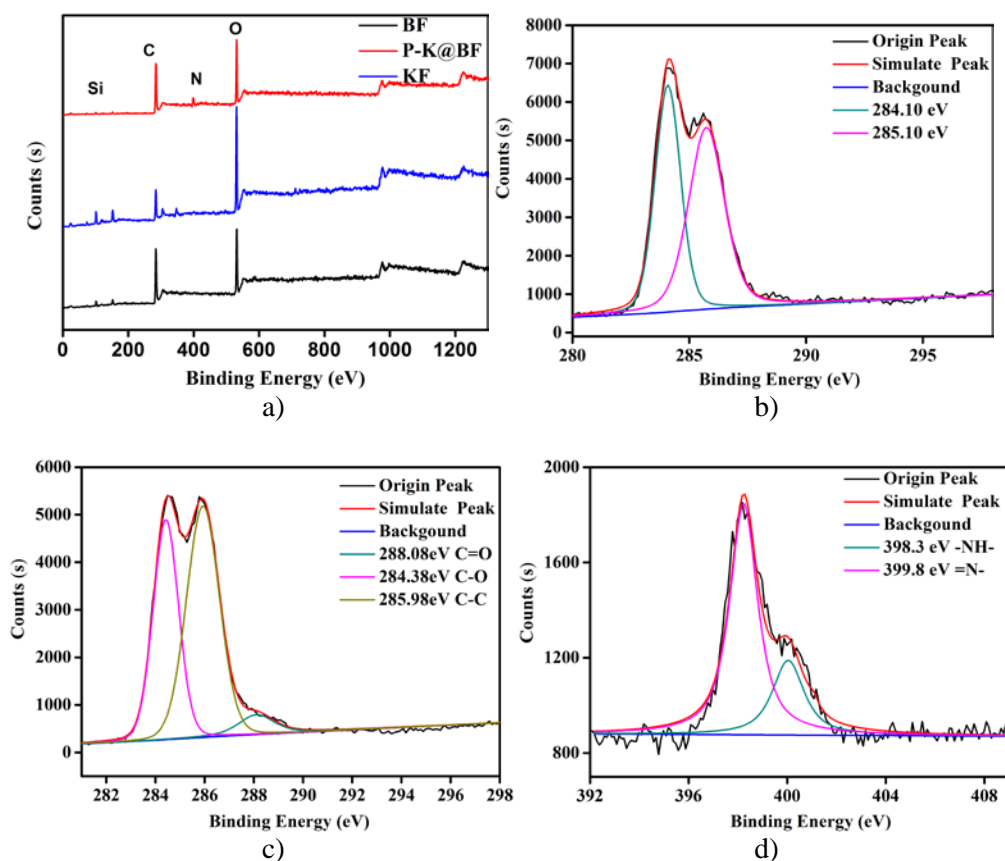


Fig. 4. (a) Overall XPS spectra of pristine BF and treated BF; (b) C 1s fitting curve of pristine BF; (c) XPS C 1s fitting curve of P-K@BF; (d) XPS N 1s fitting curve of P-K@BF.

The interfacial properties of composites are closely related to the wettability of the substrate. Measurement of the contact angle between the matrix and the reinforcement fiber is an effective method to evaluate its wettability. [40] The contact angle was measured by the Digimizer program to compare the wettability change of coatings with and without PDA-KH570@BF. The results showed that compared with the original coating, the surface of the coating with treated BF changed from hydrophobic state to hydrophilic state.

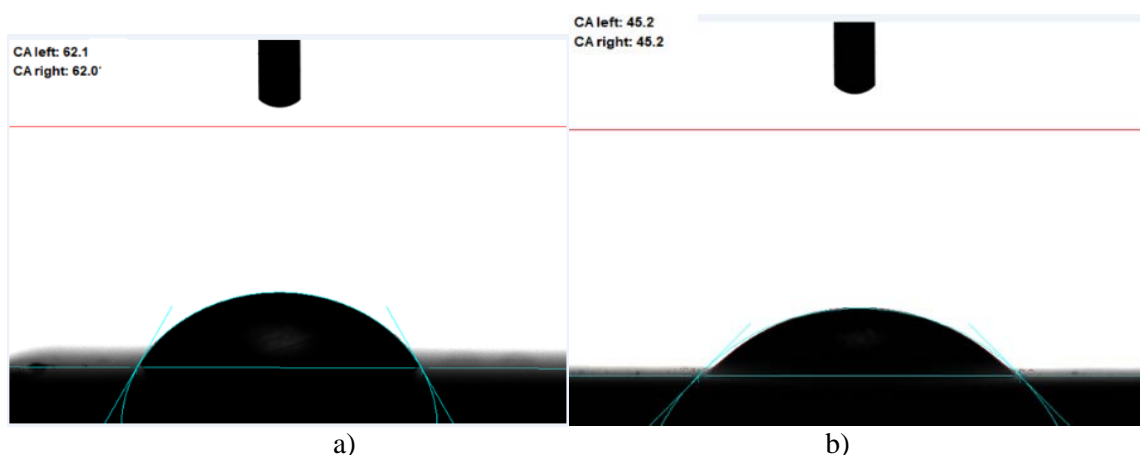


Fig. 5. Contact angle (a) the coating without filler; (b) adding the original BF at 298 K.

Fig. 5a and 5b respectively shows the contact angles of the coating and the sodium chloride solution are 62.06 ° and 45.21 ° in the case of without and with modified BF. Fig. 5a shows a higher contact angle which means that the coating has a more hydrophilic surface in the presence of modified fibers, while Fig. 6 shows a comparison of the contact angles of coatings containing different content of original BF and modified BF. By measuring the contact angle of water droplets on the coating surface, it is proved that the coating surface is more hydrophilic after addition of the original fiber, thus the contact angle of the coating decreases.

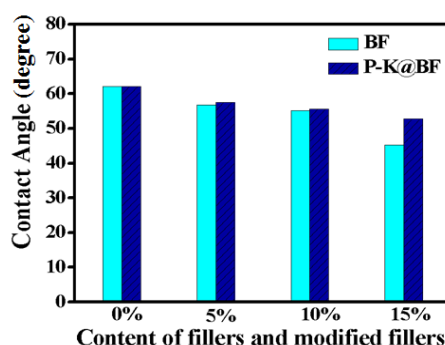


Fig. 6. Contact angle histogram of 3.5% NaCl solution on coatings with different fillers.

In addition, in Fig. 6, it can be observed that the contact angle of modified BF coating is larger than that of unmodified BF coating, indicating that the modification process makes the coatings more hydrophobic than before modification. In theory, this hydrophilic surface will have a negative effect, which is not conducive to corrosion protection, on the surface of the substrate and protects metals from corrosion. But this surface still provides better protection for metal carbon steel for the distribution of modified fibers in coatings is evenly and orderly, which prevents the spread of corrosive ions, makes the corrosion products of zinc not easy to dissolve, and also plays a significant role in protecting the substrate so as to protect the metal substrate from corrosion.

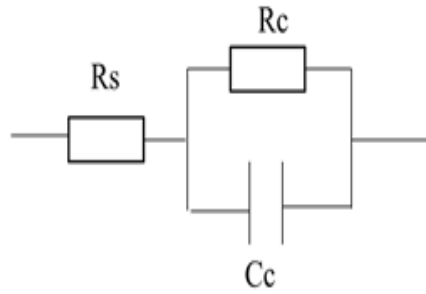
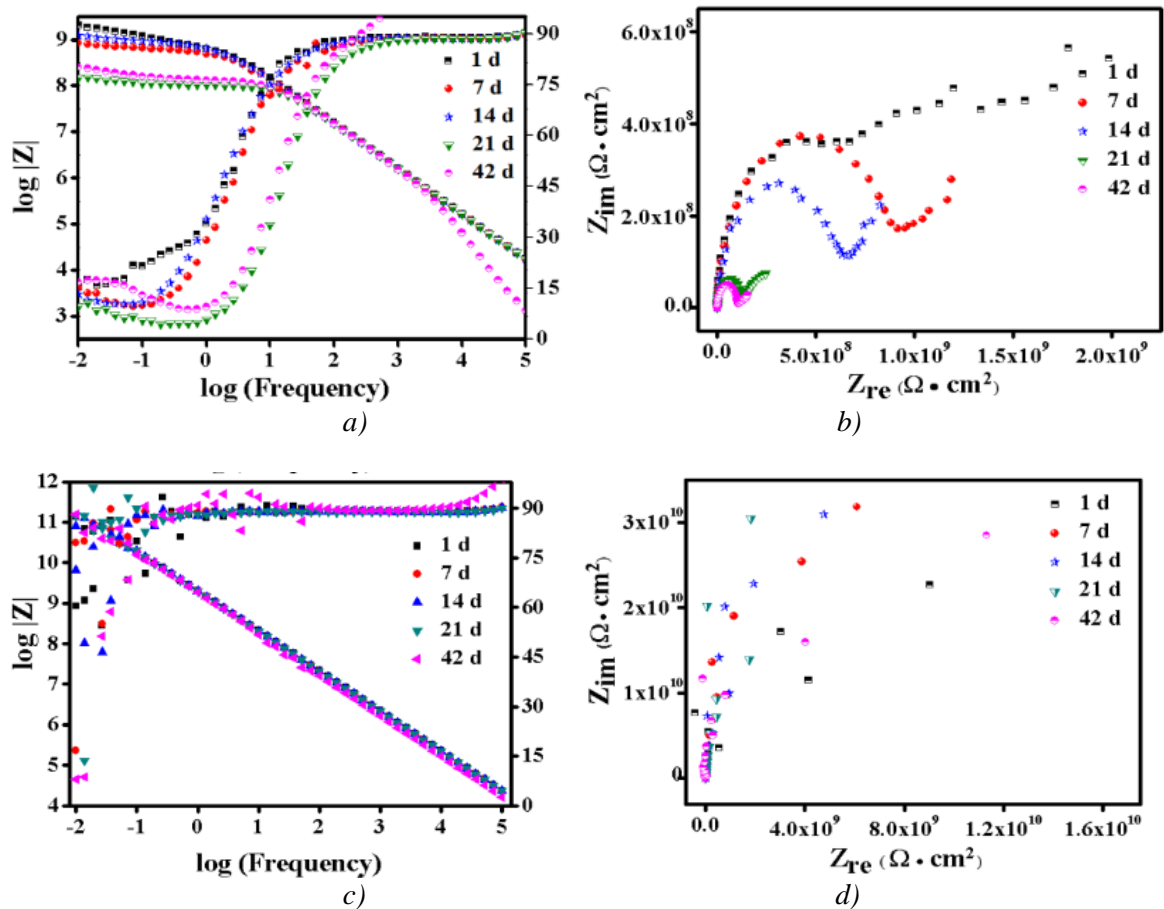


Fig. 7. Diagrams of equivalent electric circuits.

The EIS was used to measuring the charge transfer resistance ( $R_c$ ) of the corrosion process and the corrosion behavior of mild steel in different coatings. Fig. 7 is the electrical equivalent circuit diagram that is used in impedance investigation. In this diagram,  $R_s$  is the solution resistance,  $R_c$  is the charge transfer resistance and  $C_c$  is the constant phase element. Electrochemical impedance spectra for samples of Q235 steel immersed in brine with the addition of 0%, 5%, 10%, 15%, 20% of treated BF for immersion period from 1 to 42 days are presented in Fig. 8(g-h). Fig. 8(a-f) shows impedance spectra and Nyquist diagrams of the three different coatings at different immersion times, pure epoxy coating, coating with BF added and the coating added PDA-KH570@BF, coating 1, 2 and 3 correspond to each other. All of these coatings act as a barrier initially time and so their impedance modulus  $|Z|$  is the highest. But with the elapsed of time, water and electrolyte penetrate gradually into the coating and cause the coating resistance to decrease gradually.



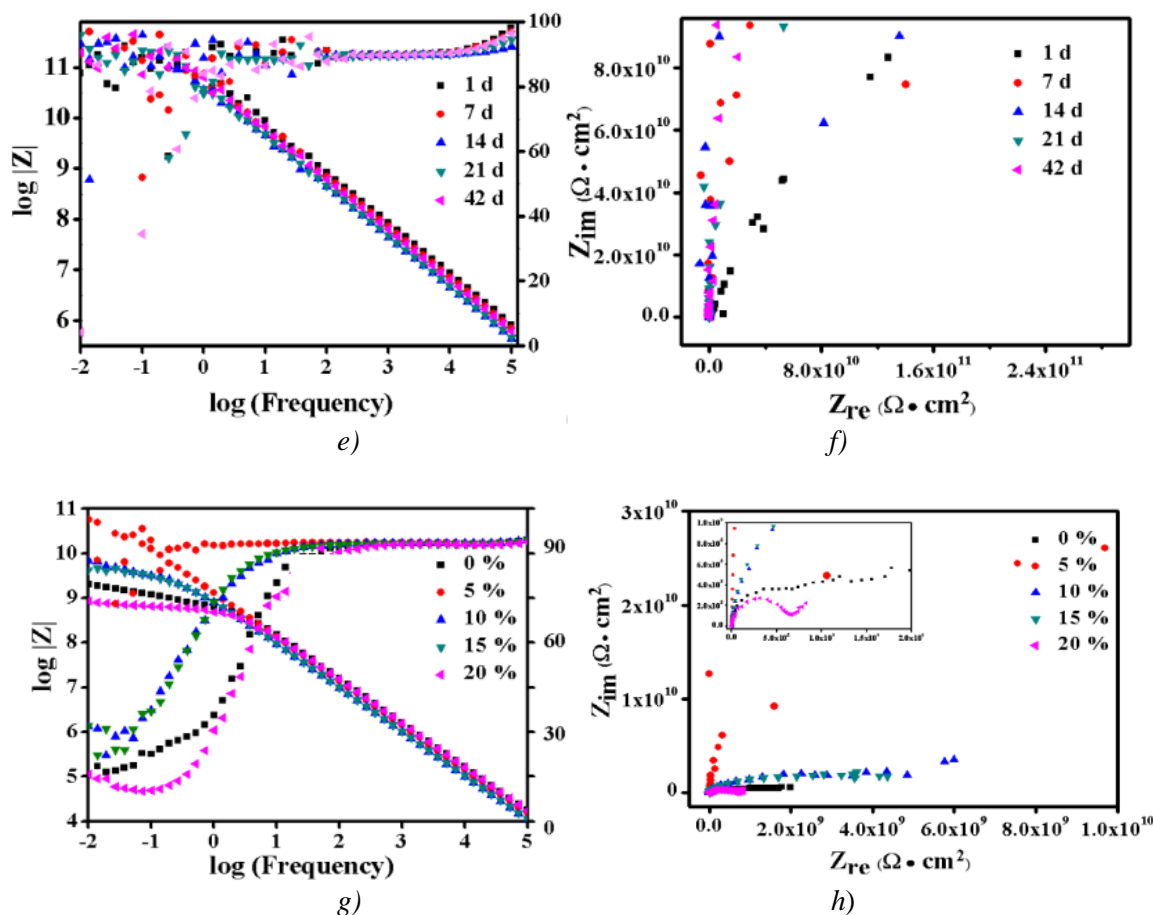


Fig. 8. Impedance spectra and Nyquist diagrams of the different coatings at different immersion times; (a, b) Pure epoxy; (c, d) 5% KH570@BF coating; (e, f) 5% PDA-KH570@BF coating; (g, h) different content of PDA-KH570@BF coating.

From Fig. 8a, it was observed that the  $|Z|$  of coating 1 decreased the fastest and the largest extent, even to about  $108 \text{ cm}^2$ . However, the initial impedance modulus  $|Z|$  of coatings 3 can reach about  $1011 \text{ cm}^2$  and remained after 42 days or even longer duration of brine immersion (Fig. 8c and e). These results reveal that the coating anti-corrosion property can be improved by adding the modified fiber, but regularity can be observed in Fig. 8e: when the modified fiber content improves, the anti-corrosion of the coating will be decreased. For the all coatings, the phase angle diagram remains almost horizontal which indicates that there is only one time constant during the immersion, the coating acts as a capacitor and has a good barrier ability for the substrate. While the phase angle of the pure epoxy coating decreased with immersion time, they began present two time constants. But the coating added 5% of modified fibre resistance also remained at  $1010 \text{ cm}^2$  and has a better anti-corrosion ability than other coatings, though its phase angle decreased. Fig. 8 (b d f h) shows Nyquist diagrams for several coatings. Fig. 8c is for coating which added 5% modified BF, its impedance changed a little and there is only one time constant: it gives good protection to the metal. With increasing immersion time, they all showed two time constants. This illustrates that the electrolyte solution has become saturated in the coatings and that the solution has reached the coating/metal interface and that corrosion has occurred. The short BF content is different in the coatings, from Fig. 8f, after the content is more than 5%, the higher content leading to lower protection for the metal. So the impedance of the coating which added 5% modified BF is higher than the other coatings. The higher pigment content enhances the defects of the coating. When the coating has been submerged in the electrolyte solution for a long time, these micro-defects can easily come into effect and the channels let the electrolyte solution penetrate from the coating to the metal surface and lead to the metal corrosion. The mechanism of the coating is the corrosion product

is difficult dissolve to water and it can block the channel which water can penetrated to the substrate and then erode the substrate. The higher basalt fiber content, the higher micro-defects are in the coating. Once the water penetrates through the surface of the coating, it will more easily get to the interface of coating/substrate along the micro-defect. In order to get the better result, the content of the fiber must be adjusted or else choose anti-corrosion pigment adding to the coating.

#### 4. Conclusions

This study investigated that the composite coating not only compact structure and high bonding strength, but also has good wear-resistance and anti-corrosion properties. The hardness and adhesion of the coating will be improved when the coating containing high content of fiber. But when the fiber content improves, the anti-corrosion of the coating will be decreased. When the coating has more than 5% fiber, its anti-corrosion property will decrease, though it has good mechanical properties. The next step work is going to adjust the content of the fiber and the zinc powder in the coating or else choose other anti-corrosion pigment substitute in order to improve the coating anti-corrosion property. The conclusions section should come in this section at the end of the article, before the acknowledgements.

#### Acknowledgements

This research was supported by Research Fund of Zhe Jiang Institute of Mechanical & Electrical Engineering (A—0271—20—211).

#### References

- [1] :Hussain, Z . Tahir, S. Mahmood, K. Ali, A . Arshad, MI . Ikram, S. Nabi, MAU .Ashfaq, A Rehman, UU. Uddassir, Y., Dig. J. Nanomater. Bios. **15**, 873 (2020).
- [2] Li, Y. H.; Chen, N.; Zhang, H. L., Dig. J. Nanomater. Bios. **13**, 491 (2018).
- [3] Shanmugasundaram, A.; Uvaraja, V. C.; Ramesh, G. Dig. J. Nanomater. Bios. **14**, 407 (2019).
- [4] R. David, V. S. Raja, S. K. Singh, P. Gore, Prog. Org. Coat. **120**, 58 (2018).
- [5] M. Müller, P. Valášek, A. Rudawska, R. Chotěborský, J. Adhes. Sci. Technol. **32**, 1531 (2018).
- [6] Y. Wang, L. Zhu, J. Zhou, B. Jia, Y. Jiang, J. Wang, M. Wang, Y. Cheng, K. Wu, Polym. Bull. **76**, 3957 (2019).
- [7] B. Demir, K. M. Beggs, B. L. Fox, L. Servinis, L. C. Henderson, T. R. Walsh, Compos. Sci. Technol. **159**, 127 (2018).
- [8] Y. Shi, B. Yu, Y. Zheng, J. Yang, Z. Duan, Y. Hu, J. Colloid Interface Sci. **521**, 160 (2018).
- [9] A. A. Premnath, J. Nat. Fibers, **1** (2018).
- [10] M. Zhong, Y. Zhang, X. Li, X. Wu, Surf. Coat. Technol. **347**, 191 (2018).
- [11] Metro, M. M.; Selvaraj, M., Dig. J. Nanomater. Bios. **15**, 953 (2020).
- [12] C. Arslan, M. Dogan, Composites, Part B **146**, 145 (2018)
- [13] B. Benmokrane, F. Elgabbas, E.A. Ahmed, P. Cousin, J. Compos. Constr. **19**, 04015008 (2015).
- [14] V. Fiore, T. Scalici, G. Di Bella, A. Valenza, Compos. Part B **74**, 74 (2015).
- [15] M. R. Ricciardi, I. Papa, V. Lprestò, A. Langella, V. Antonucci, Compos. Struct. **214**, 476(2019).
- [16] S. Yu, K.H. Oh, J.Y. Hwang, S. H. Hong, Compos. Part B **163**, 511 (2019).
- [17] C. Ralph, P. Lemoine, A. Boyd, E. Archer, A. McIlhagger, Appl. Surf. Sci. **475**, 435 (2019).
- [18] S. Liu, G. Wu, J. Yu, X. Chen, J. Guo, X. Zhang, P. Wang, X. Yin, Compos. Interfaces **26**, 275(2018).

- [19] P. Miśkiewicz, I. Frydrych, W. Pawlak, A. Cichocka, Cichocka, Res. J. **19**, 36 (2019).
- [20] X. Wang, X. Zhao, Z. Wu, Mater. Des. **163**, 107529 (2019).
- [21] Y. Li, Z. Li, J. Wan, Z. Yan, J. Sun, S. Zhao, Polym. Compos. **40**, 630 (2017).
- [22] M. N. Roslan, M. Y. Yahya, Z. Ahmad, A. H. A. J. Phys.: Conf. Ser. **1150**, 012048 (2019).
- [23] S. Kuciel, P. Romańska, Mater. **12**, 95 (2018).
- [24] V. Dhand, G. Mittal, K. Y. Rhee, S.-J. Park, D. Hui, Compos. Part B **73**, 166 (2015).
- [25] M. Zhu, J. Ma, Appl. Surf. Sci. **464**, 636 (2019).
- [26] S. E. Vannan, Miner. J. Mater. Charact. Eng. **3**, 289 (2015).
- [27] X. Liu, P. Hou, X. Zhao, X. Ma, B. Hou, J. Coat. Tech. Res. **16**, 71 (2018).
- [28] S. V. Tkachev, S. V. Kraevskii, D. Y. Kornilov, V. A. Voronov, S. P. Gubin, Inorg. Mater. **52**, 1254 (2016).
- [29] Z. Chen, Y. Huang, J. Adhes. Sci. Technol. **30**, 2175 (2016).
- [30] R. Huang, C. Mei, X. Xu, T. Karki, S. Lee, Q. Wu, Mater. (Basel) **8**, 8510 (2015).
- [31] L. Luo, Q. Ma, Q. Wang, L. Ding, Z. Gong, W. Jiang, Coatings **9**, 154 (2019).
- [32] N. Jamali, A. Rezvani, H. Khosravi, E. Tohidlou, Polym. Compos. **39**, E2472 (2018).
- [33] P. Lacki, A. Derlatka, J. Compos. Struct. **218**, 60 (2019).
- [34] R. Kaundal, A. Patnaik, A. Satapathy, J. Mater.: Des. Appl. **232**, 893 (2016).
- [35] G.-H. Wu, S.-Q. Liu, X.-Y. Wu, X.-M. Ding, J. Polym. Res. **23**, 155(2016).
- [36] Y. Zhou, J. Yu, X. Wang, Y. Wang, J. Zhu, Z. Hu, Fibers Polym. **16**, 1772 (2015).
- [37] L. Chen, Y. Wang, D. Zia Ud, P. Fei, W. Jin, H. Xiong, Z. Wang, Int. J. Biol. Macromol. **104**, 137(2017).
- [38] Y. Min, Y. Fang, X. Huang, , Y. Zhu, W. Li, J. Yuan, L. Tan, S. Wang, Z. Wu, Appl. Surf. Sci. **346**, 497 (2015).
- [39] Y. Mao, S. Zhang, W. Wang, D. Yu, Colloids Surf. A **558**, 538 (2018).
- [40] X. Wang, S. Zhai, K. Wang, T. Xie, Compos. Interfaces **25**, 27 (2017).